

## MECHANICAL EFFECTS ON ELECTRODE DURING PLASMA CUMULATION NEAR THE AXIS

S. K. GODUNOV, N. V. FILIPPOV, and T. I. FILIPPOVA

Submitted to JETP editor November 22, 1966

J. Exptl. Theoret. Phys. (U.S.S.R.) 52, 1138-1145 (May, 1967)

Brief contact between a gas discharge plasma at over  $10^7$  °K and a metallic electrode not only results in intensive evaporation of the surface but in some cases, owing to the high pulsed pressures which may be as high as several megabars, leads to shock-wave destruction of the external side of the electrode i.e. to rear end splintering. A deuterium plasma with an energy content sufficient to produce such pulsed pressures for a period of  $\sim 10^{-7}$  sec has been obtained by noncylindrical compression of a z-pinch<sup>[1]</sup>. The splintering phenomenon is used in the present study in an attempt to determine the pulsed pressure (or energy content) in the plasma focus. For this purpose, calculations are carried out for a model planar problem involving passage of a shock wave through an aluminum plate and reflection of the wave from a free boundary. The dependence of the thickness of the splintered layer on the pressure amplitude is found for a given pulse shape corresponding to a prescribed duration. An analysis of the experimental results, based on the calculations, shows that the energy density on the plasma focus may reach  $10^{23}$ – $10^{24}$  eV/cm<sup>3</sup>, in agreement with other independent estimates. Thus the splintering method can be employed for diagnostics of dense hot plasmas.

**A**MONG the numerous topics investigated in the field of controlled thermonuclear fusion are rapid pulsed processes capable of producing and heating a deuterium plasma to temperatures of tens of millions of degrees. The simplest example of such a rapid process is the linear z-pinch, studied in the USSR and in the USA as early as in 1952.

The apparatus with which the research was carried out constituted a high-voltage capacitor bank discharging into a cylindrical chamber of ceramic or glass. The metallic ends of the chambers served as electrodes (the cathode and anode were identical in shape). A current exceeding  $10^6$  A with a growth rate up to  $10^{12}$  A/sec was passed through the chamber, which was filled with hydrogen or deuterium at a pressure  $10^{-1}$ – $10^{-2}$  mm Hg. Such systems were the first to yield pulsed neutron and hard x-radiation from a plasma. Numerous experimental investigations yielded some ideas concerning the mechanisms of formation, development, and decay of the pinch column. It became clear at the same time that an increase in the energy stored in the battery, beyond a certain limit characteristic for each given setup, does not increase the neutron yield, but to the contrary, suppresses all of the hard radiation from the discharge. It was assumed that the main cause limiting the attainable temperatures and energy content of the plasma is evaporation of the low-thermal-conductivity ceramic chamber walls

during the emission stage of discharge formation.

Figure 1 shows the construction of one variant of a gas-discharge chamber which is practically free of this shortcoming. The chamber consists of a copper housing, 3, which serves as a cathode, and a positive electrode, 5, of 480 mm diameter, introduced through a porcelain insulator. Capacitor bank, 1, are rated  $180 \mu\text{F}$  at a working voltage of 24 kV was discharged into the chamber through a vacuum switch, 2. The channel was filled with deuterium to a pressure of  $\sim 1$  Torr. The current through the chamber and the voltage on it were measured with an oscilloscope using integrating Rogowski loop and an ohmic divider, 6. The operating principle and the characteristic of development of the discharge were described in detail in<sup>[1-3]</sup>.

The difference in the geometric shapes of the anode and the cathode changes the character of contraction of the discharge towards the chamber axis, making it non-cylindrical. During the initial stage of the discharge, the current sheath is formed, just as in cylindrical chambers, near the surface of the insulator, but it then moves not towards the axis but to the side walls of the chamber. The motion of the gas towards the center of the chamber proceeds along the surface of the internal (positive) electrode and begins after the current has grown practically to a maximum. The gas in which the initial stage of the development of the

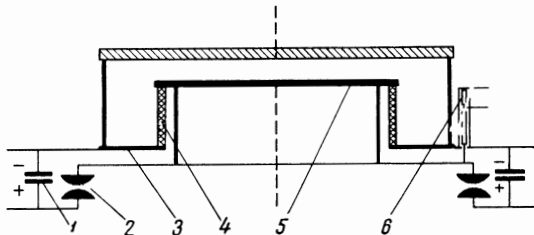


FIG. 1. Diagram of gas-discharge chamber: 1 – Capacitor bank, 2 – vacuum switch, 3 – chamber housing, 4 – porcelain insulator, 5 – anode, 6 – ohmic divider.

discharge took place does not participate in the compression.

The main phase of the discharge is the contraction of the sheath towards the axis under the influence of the electrodynamic forces, and is characterized by formation of a shock wave, which plays a stabilizing role during the motion. The singularities of the investigated type of compression, connected with the non-cylindrical shape of the sheath, appear during the same phase of the discharge. Leakage of the “swept up” gas along the plasma layer is observed and increases in time. This leads to an appreciable increase in the radial velocity of the contraction of the sheath near the electrode. Cumulation on the chamber axis, produces within a short time interval  $((1-2) \times 10^{-7}$  sec) a plasma focus with a particle temperature exceeding 1 keV and a density exceeding  $10^{19}$  cm $^{-3}$ . When the chamber is filled with deuterium, the plasma focus serves as a sharply localized source of neutrons of strength up to  $10^{10}$  neut/pulse. The concentration of the energy can in this case exceed  $10^{22}$  eV/cm $^3$ , and should become manifest as a pulsed pressure on the electrode, since the kinetic energy of the sheath goes over at this instant into the energy of random motion.

The high plasma parameters and the complexity of the geometric shape, the latter aggravated by the small dimensions of the compression focus, make it difficult to employ usual diagnostics methods, but at the same time uncover new interesting possibilities. In particular, the pulsed pressure on the chamber axis becomes large enough to lead in many cases to the appearance of “rear-end splintering”<sup>1)</sup> of the chamber electrode material. In this paper we present results of experiments with “splintering” and attempt to use this phenomenon to estimate the energy density in the plasma focus.

<sup>1)</sup>The “splintering” method is used to investigate the compressibility of solids up to pressures  $\approx 4 \times 10^6$  atm and to determine the parameters of shock-wave fronts [4].

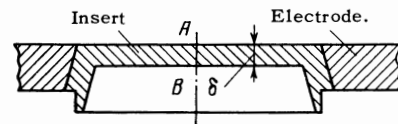


FIG. 2. Construction of insert.

Figure 2 shows the construction of the removable insert, used to observe the splintering, of the central part of the positive electrode. Regions A and B are respectively the internal and external parts of the discharge chamber. The insert materials and the thickness  $\delta$  of the working part were varied from experiment to experiment.

Figure 3 shows a typical photograph of the surface (A) of the electrode subjected to the pulsed action of the plasma, while Fig. 4 shows a picture of the splintering as observed from the external side of the electrode. The thickness of the duraluminum insert was in this case 6 mm, and the thickness of the splintered layer was 0.5–0.7 mm. A trace of the contact between the pinch and the electrode, in the form of a molten crater of  $\sim 1$  mm diameter and having approximately the same depth, is located in the center of the surface section on which the plasma acted. Unfortunately, reflections of the metal on the photograph make it difficult to see the crater. Splinters of thickness from 0.1 to 0.7 mm were observed at different discharge conditions and when the thickness of the insert was varied. The area of the splinter turned out to be variable, ranging from 2 to 200 mm $^2$ .

The rate of scattering of the splintering material was determined by high speed photography and exceeded in some cases 2 km/sec. In most cases, the splintered layer broke up into minute fragments. In weaker reactions, swelling of the material was observed in lieu of splintering. It was then possible

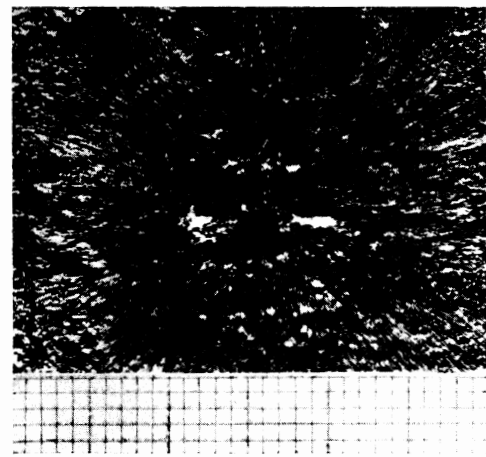


FIG. 3. Internal surface of insert which is in contact with the plasma.

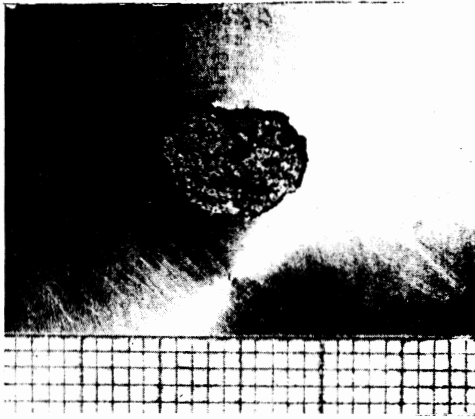


FIG. 4. Photograph of splinter.

to trace the character of formation of the crack transverse to the direction of wave propagation. The crack development terminated in splintering of the thin layer of material. A metallographic microphotograph of a polished transverse section of the insert near the crack is shown in Fig. 5. The thickness of the splinter was in this case  $\sim 0.6$  mm, and the length of the crack was  $\sim 4.3$  mm. Measurements were made of the microhardness over the cross section of the sample in the direction of shock wave propagation. The distribution of the hardness was uneven; the hardness of the section that has peeled off from the zone adjacent to the crack exceeded the microhardness of the main sample by approximately 10%. Figure 5 reveals the existence of longitudinal microcracks, which are probably the consequence of the increasing brittleness of the material in the region of the deformation.

In order to calculate the dimensions and the velocity of the splinters as a function of the ampli-

FIG. 5. Microphotograph of structure of cross section of a duraluminum insert (100 $\times$ ).

tude of the applied pressure and of its duration, we carried out calculations for a model planar problem. We traced the passage of a shock wave due to an applied pressure pulse through a plate made of duraluminum, and also the reflection of this wave from the free boundary of the plate. Reflection gives rise to a rarefaction wave with a very sharp pressure gradient and with large negative (tensile) stresses. The resultant stresses can lead to the splintering<sup>[4]</sup>.

In solving the problem, we used the experimentally obtained characteristic times of existence of the extremal conditions in the pinch (0.1  $\mu$ sec), and specified, on the basis of theoretical calculations<sup>[5]</sup>, the order of magnitude of the pressure in the pinch during that time. The pressure was varied subsequently within reasonably broad limits. It was convenient to assume in the calculations that the pressure pulse has an infinitely steep leading front and an exponentially decreasing trailing front.

In the calculations we used as the velocity unit a value  $10^5$  cm/sec, the length unit was 1 cm, and the unit time was  $10^{-5}$  sec. In terms of these units, the problem of pulsed pressure in the pinch is formulated in the following fashion:

On the right edge of a plate of thickness 0.4 there is applied a pressure

$$p = p_0 e^{-100t}; \quad (1)$$

The pressure amplitude  $p_0 = 5$  corresponds, in units that are convenient for plasma experiments, to a pinch energy density  $3.12 \times 10^{22}$  eV/cm<sup>3</sup>.

The equation of state of the matter in the plate is written in the form usually employed for solids<sup>[4]</sup>:

$$p = \frac{\rho_0 c_0^2}{\gamma} \left[ S \left( \frac{\rho}{\rho_0} \right)^\gamma - 1 \right], \quad (2)$$

where  $S$  is the entropy variable,  $\gamma = 7/3$ ,  $\rho_0 = 2.71$ ,  $c_0 = 5.5$  ( $c_0$ —speed of sound). The chosen constants correspond to the physical conditions under consideration.

On Hugoniot adiabat, the following expression is used for the energy:

$$E = 1/2 p (1/\rho_0 - 1/\rho). \quad (3)$$

Figure 6 shows in  $(x, t)$  coordinates the motion of the shock wave (1), of the free boundary (2), of the compressed boundary (3), and of the characteristics bounding the rarefaction wave (4, 5). The boundary to which the pressure is applied was calculated up to  $t = 0.0690$ , that is, up to the instant of emergence of the shock wave to the free boundary of the plate. Following this instant, the motion was calculated only for the part of the plate

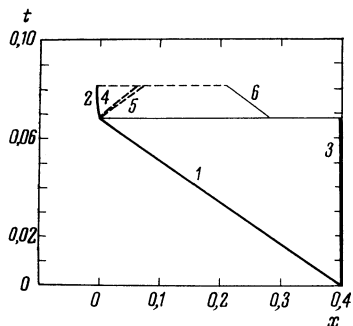


FIG. 6. Plot of shock-wave motion (from right to left), of the free and compressed boundaries, and of the characteristics bounding the compression wave.

adjacent to the free boundary and bounded on the right by the characteristic  $dx/dt = u - c$  [(6) in the same figure]. The assumed limitation makes it possible to reduce greatly the volume of the calculations, but does not introduce additional approximations in the calculation of the phenomena of interest to us.

Figure 7 shows the variation of the pressure along the shock wave. During the time of passage of the wave, the amplitude of the pulse decreased only from 5 to 3.8, although the pressure on the right-hand boundary decreased during that time by approximately  $e^7$  times. Such an insignificant decrease in the amplitude is due to the fact that the wave corresponding to the initial pressure 5 is very weak—almost sonic.

Figure 8 shows the distributions of the velocities and of the pressures in the plate at the instant  $t_1 = 0.0690$  when the shock wave emerges from the left boundary.

Figure 9 shows the characteristic distribution of the pressures in the plate in the presence of a wave reflected from the left-hand boundary—rarefaction wave. It is seen that the maximum tensile stress is reached on the characteristic  $dx/dt = u + c$ , which bounds the rarefaction wave from the left.

Figure 10 shows the time variation of the maximum tensile stress. It is seen from the figure that the critical stress (from the point of view of strength), equal to 2, is reached at  $t \approx 0.075$ , when the characteristic is approximately 0.40 mm away from the boundary. The splintered layer should be of approximately the same thickness.

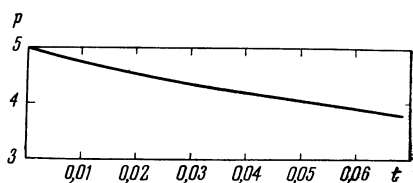


FIG. 7. Variation of pressure along the shock wave.

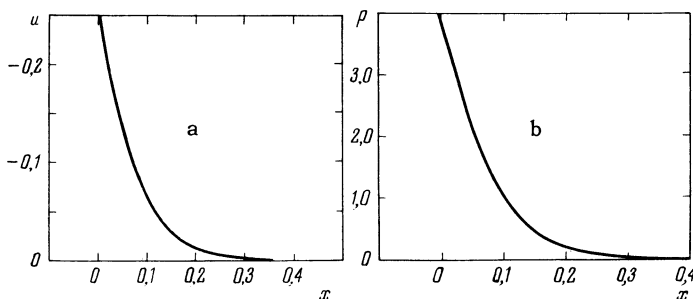


FIG. 8. Distribution of velocities (a) and pressures (b) at the instant  $t_1 = 0.0690$  (emergence of wave to the left boundary).

The calculations were made by a finite-difference method, using moving nets in each of the regions into which the problem was broken up by the moving boundaries (shock waves and characteristics). Steep gradients called for smaller differences both in space and in time. The time interval was chosen to be  $\tau = 0.0002$ . In the calculation of the passage of the wave, 99 points were used between the wave and the right-hand boundary. In the calculation of the reflected rarefaction wave, 30 calculation points were used inside the wave.

Let us see now how the tensile stresses are produced on the characteristic  $dx/dt = u + c$  which emerges from the left boundary ( $x_1$ ) at the instant when the shock wave arrives at this boundary (see Fig. 6). At the instant  $t = t_1$  (emergence of shock wave), the quantities  $u$ ,  $c$ , and  $\rho$  can be assumed to have a linear distribution with respect to the coordinate  $x$  near the left-hand boundary. In particular, the quantity  $u - 2c/(\gamma - 1)$  is assumed to be linear in  $x$ :

$$u - \frac{2}{\gamma - 1}c \Big|_{t=t_1} = \alpha_0 + \alpha_1[x - x_1(t_1)]. \quad (4)$$

The coefficients  $\alpha_0$  and  $\alpha_1$  of this linear function can be taken from the plots obtained as a result of calculation of the motion of the shock wave.

Since  $u - 2c/(\gamma - 1)$  is a Riemann invariant, that is, it is conserved along the characteristics  $dx/dt = u - c$ , we obtain for it (when  $t \geq t_1$ ) the following approximate formula:

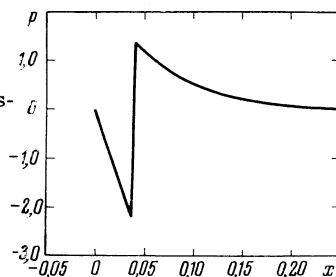


FIG. 9. Distribution of pressures in the presence of a reflected wave.

$$u - \frac{2}{\gamma - 1}c = \alpha_0 + \alpha_1[x - x_1(t) - (u - c)_{x_1 t_1}(t - t_1)]. \quad (5)$$

In the derivation of this formula we neglected the variation in the slope of the characteristics  $u - c$ , and assumed that

$$u - c \equiv (u - c)_{x_1 t_1}. \quad (6)$$

When the shock wave emerges from the left boundary, a rarefaction wave is produced, consisting of a narrow bundle of characteristics  $dx/dt = u + c$  (see Fig. 6, where the left (4) and right (5) characteristics of the bundle are marked). We are interested in the quantities on the left-hand characteristic. The value  $(u + c)_{t_1}$  on this characteristic can be determined only from the shock wave parameters at the instant of its emergence from the boundary. We determine the value of  $[u + 2(\gamma - 1)^{-1}c]_{t_1}$  on this characteristic in exactly the same way. Such a combination of the velocity of matter and the speed of sound is a Riemann invariant for this characteristic, and remains constant along it.

Thus, we can assume approximately that the following relations hold along the left-hand characteristic:

$$u + \frac{2}{\gamma - 1}c = \left(u + \frac{2}{\gamma - 1}c\right)_{x_1 t_1}, \quad (7)$$

$$x - x_1(t_1) = (u + c)_{x_1 t_1}(t - t_1). \quad (8)$$

From this and from (5) we see, that at the assumed accuracy,  $c$  will be a linear function of the time along the characteristic, and its parameters will depend on the parameters of the shock wave at the instant of its emergence from the boundary, and on the gradients of the quantities  $u$  and  $c$  behind the front of the wave at that same instant. In the isentropic case, the pressure  $p$  can be determined from the known value of  $c$  with the aid of (2).

The decrease of the pressure and velocity behind the front of the wave leads to a decrease in the pressure along the characteristic  $dx/dt = u + c$ . Since the pressure on the left characteristic of the bundle is equal to zero at the instant of the forma-

tion of the rarefaction wave, its decrease leads to the occurrence of tensile stresses.

We have also calculated variants with variable pressure amplitude:

$$\begin{aligned} p &= 15e^{-100t}, & p &= 25e^{-100t}, \\ p &= 40e^{-100t}, & p &= 50e^{-100t} \end{aligned} \quad (9)$$

and obtained for them approximate formulas for the velocity of  $c$  along the characteristics with maximal tensile stress:

$$c = \beta_0 + \beta_1(t - t_1), \quad (10)$$

$$c = \delta_0 + \delta_1(x - x_1). \quad (11)$$

Here

$$\begin{aligned} x - x_1 &= [x - x_1(t_1)] - u_1(t - t_1) \\ &= [(u + c)_{x_1 t_1} - u_1(t_1)](t - t_1). \end{aligned} \quad (12)$$

The values of the coefficients are listed in the table for a pulse in the form  $p = p_0 \exp(-100t)$ .

If we assume that the splintering occurs at a critical stress  $p_{cr} = -2.0$  and  $c_1 = 5.341$ , then we obtain for the thickness of the splintered layer  $\Delta x = (x - x_1)|_{c=c_1}$ , as a function of the pressure amplitude, the following values<sup>2)</sup>:

$p_0$ :	5	15	25	40	50
$\Delta x$ , mm:	0,4	0,32	0,26	0,22	0,20

The amplitude of a pressure equal to 5 corresponds to an energy density in the plasma  $3.12 \times 10^{22}$  eV/cm<sup>3</sup> (in the case of a plane-front shock wave).

In the general case the thickness of the fragmented layer depends much strongly on the duration of the pressure pulse ( $\Delta x = c\Delta t$ ) than on its amplitude. The very fact that the splinter is produced yields a lower-bound estimate for the pressure. In the opposite case, when no splintering is observed, the same reasoning yields an upper bound for  $p$ .

From an analysis of the data presented for  $\Delta x$  it follows that the discussed measurement method has maximum sensitivity at a pressure on the order of critical. With increasing  $p$ , the  $\Delta x(p)$  dependence exhibits saturation. However, at the same time, the velocity with which the splintered layer travels increases. All the excess energy of the compressed solid, with the exception of the work connected with the disintegration of the material, goes over into the kinetic energy of the fragment. If we measure in each experiment both the thickness and the velocity of the fragment, then the accuracy with which  $p$

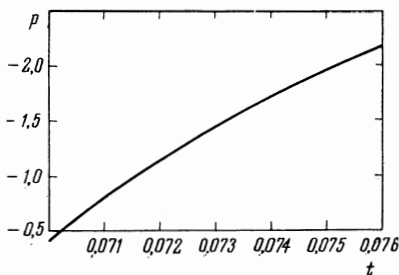


FIG. 10. Time variation of the maximum tensile stress.

<sup>2)</sup>We include also the accurately-calculated  $\Delta x$  for  $p = 5 \exp(-100t)$ .

$p_0$	$\beta_0$	$\hat{p}_1$	$\delta_0$	$\delta_1$	$p_0$	$\beta_0$	$\hat{p}_1$	$\delta_0$	$\delta_1$
15	5.501	-27.7	5.501	-5.04	40	5.508	-42.5	5.508	-7.71
25	5.503	-34.5	5.503	-6.26	50	5.513	-46.2	5.513	-8.38

is determined greatly increases and the method can be extended to include values  $p \gg p_{\text{crit}}$ .

For the concrete example chosen, the action of the plasma on the electrode lasted approximately  $10^{-7}$  sec and the thickness of the splintered layer was approximately 0.4 mm and its velocity approximately  $1 \times 10^5$  cm/sec. All these quantities can be reconciled if the pressure amplitude is taken to be 5–15, that is,  $(3-10) \times 10^{22}$  eV/cm<sup>3</sup>, and if the wave front is assumed plane. Additional corrections to the pressure amplitude should be introduced when account is taken of the almost pointlike contact between the plasma focus and the electrode.

Comparison of Figs. 3 and 4 indicates that a correction coefficient must be introduced to account for the difference in the area of the splinter and the area of the contact between the plasma and the electrode. (The wave is not plane but almost spherical.) In our case this coefficient can range approximately from 30 to 100. Since the wave is not strong, almost sonic, the ratio of the areas increases by a corresponding number of times the amplitude of the pressure at the focus of the plasma compression, that is, the concentration of the energy obtained during the cumulation approaches  $10^{24}$  eV/cm<sup>3</sup>.

Thus, the method of "rear-end splintering" can be used as an independent and rather illustrative method of determining the pulsed motion of the plasma to an electrode in those cases when this pressure is too large for ordinary measurement methods (piezoceramics, quartz, etc.). A suitable choice of materials for the insert and the electrode can reduce the critical amplitude of the pressure that leads to splintering.

The first experiments of this type were carried out by the authors in an investigation of ordinary cylindrical discharges. A small cylinder of chalk, of 8 mm diameter and 5 cm length, was suspended freely in the center of a porcelain chamber, flush with the surface of the lower electrode. The pulsed action of the pinch in the compressed state caused

a tablet 4 mm thick to splinter off the end of the chalk bar. The pulsed pressure of the plasma was insufficient to splinter stronger materials in this case.

The question of the nature of the pressure profile which is specified in the calculation calls for further analysis; in particular, it is necessary to consider the contribution of the momentum of the evaporating material of the electrode at the place where contact is made with the plasma. However, even when the momentum is increased by the evaporation by ten times the computed energy content of the plasma will not decrease below  $10^{23}$  eV/cm<sup>3</sup>.

In conclusion, the authors thank V. S. Imshennik for taking part in the organization of the work and a discussion of the result, and M. D. Takhtamyshev and L. A. Pliner for taking part in the calculations.

The authors are also grateful to Yu. I. Konnov and E. G. Ivanov for taking the microphotographs.

<sup>1</sup>N. V. Filippov, T. I. Filippova, and V. P. Vinogradov, Nuclear Fusion Suppl. part 2, p. 557 (1962).

<sup>2</sup>N. V. Filippov and T. I. Filippova, Plasma Phys. and Controlled Nucl. Fusion Res., Culham, 1965, 2, p. 405.

<sup>3</sup>Yu. A. Kolesnikov, N. V. Filippov, and T. I. Filippova, Proc. of the 7th Intern. Conf. on Ioniz. Phenom. in Gases, Belgrade, 1965, Paper 4.7.29.

<sup>4</sup>Ya. B. Zel'dovich and Yu. P. Raizer, Fizika udarnykh voln i vysokotemperaturnykh gidrodinamicheskikh yavlenii (Physics of Shock Waves and High-temperature Hydrodynamic Phenomena. Nauka, 1966.)

<sup>5</sup>V. F. D'yachenko and V. S. Imshennik, Zh. vychisl. matem. i matem. fiz. (J. of Comput. Math. and Math. Phys.) 3, 915 (1963).

Translated by J. G. Adashko